

# Bond-Stretch Isomerism in Tetrasilabicyclo[1.1.0]butane Derivatives

Jerry A. Boatz\*

Phillips Laboratory, Propulsion Sciences Division, OLAC PL/RKS,  
10 East Saturn Boulevard, Edwards AFB, California 93524-7680

Mark S. Gordon

Department of Chemistry, Iowa State University, Ames, Iowa 50011

Received October 27, 1995<sup>®</sup>

The existence of bond-stretch isomers (isomers which differ primarily in the length of the bridgehead bond) of tetrasilabicyclobutane, Si<sub>4</sub>H<sub>6</sub>, recently has been predicted using *ab initio* electronic structure methods of quantum chemistry. At the GVB/3-21G\* level of theory, the “short bond” isomer is predicted to be less stable than the “long bond” isomer. Although the parent compound has not yet been experimentally observed, the X-ray crystal structure of a heavily-substituted derivative is known. This derivative compound apparently does not exist in two bond-stretch forms; rather, only the short bond isomer is observed. The present work is an attempt to resolve the differences between the theoretical predictions for the parent Si<sub>4</sub>H<sub>6</sub> molecule and the experimental observations of the derivative compound. In particular, a systematic study of how methyl and *tert*-butyl substituents affect the relative stabilities of the two bond-stretch isomers is presented. A detailed analysis of the relative energies of the bond-stretch isomers and isomerization barriers for the parent compounds (Si<sub>4</sub>H<sub>6</sub>) as a function of basis set and theoretical method is presented.

## Introduction

Highly strained compounds with large positive heats of formation may be useful as additives to rocket propellants as a means of improving performance. Examples of such compounds include derivatives of cubane and quadricyclane. Another type of molecule which might be capable of boosting the performance of conventional propellants is tetrasilabicyclo[1.1.0]butane (Si<sub>4</sub>H<sub>6</sub>), the silicon analog of bicyclo[1.1.0]butane. This is due in part to the high heat of formation of Si<sub>4</sub>H<sub>6</sub>, which *ab initio* calculations predict to be  $\Delta H_{f,298}^\circ = 93$  kcal/mol.<sup>1</sup> Another contributing factor is the overwhelming thermodynamic stability of SiO<sub>2</sub>(s), presumably one of the primary combustion products.

Si<sub>4</sub>H<sub>6</sub> has been the focus of several theoretical studies<sup>1–9</sup> which have predicted the molecular and electronic structure, harmonic vibrational frequencies, strain energies, and enthalpies of formation of this molecule. Some of these previous papers<sup>2–6</sup> have also predicted the existence of two Si<sub>4</sub>H<sub>6</sub> “bond-stretch” isomers, which differ primarily in the distance between the bridgehead silicons. The “short bond” isomer is a

classical closed-shell species with the length of the bridgehead bond only slightly longer than a typical Si–Si single bond. The “long bond” isomer, while retaining essentially a closed-shell electronic structure, has significant singlet diradical character in the bridge bond. Similar behavior has been predicted<sup>10</sup> for related compounds.

Of further interest is the predicted energetic preference for the long bond isomer of Si<sub>4</sub>H<sub>6</sub>.<sup>2–6</sup> It appears that in the unsubstituted system the long bond isomer is indeed more stable than its short bond counterpart. However, the effect of bridgehead and peripheral substituents on the relative stabilities of the bond stretch isomers is rather unclear. Although prior theoretical studies<sup>3,4</sup> have predicted that placement of methyl groups on the bridgehead positions reverses the order of stability, these calculations did not include reoptimization of the geometries of the substituted molecules. Si<sub>4</sub>H<sub>6</sub> has not been experimentally detected, but the X-ray crystal structure of the 1,3-di-*tert*-butyl-2,2,4,4-tetrakis(2,6-diethylphenyl) derivative is known.<sup>11</sup> In this derivative, only the short bond isomer is observed. This observation suggests that substituents may have a dramatic effect on the relative energies of the bond-stretch isomers of silicon-based bicyclobutanes.

The present work is a systematic study of how alkyl bridgehead substituents affect the relative energies of the bond stretch isomers, as well as the isomerization barriers, of tetrasilabicyclobutane. In particular, the

<sup>®</sup> Abstract published in *Advance ACS Abstracts*, March 15, 1996.

(1) (a) Boatz, J. A.; Gordon, M. S. *J. Phys. Chem.* **1988**, *92*, 3037.

(b) Boatz, J. A.; Gordon, M. S. *J. Phys. Chem.* **1990**, *94*, 7331.

(2) Boatz, J. A.; Gordon, M. S. *J. Phys. Chem.* **1989**, *93*, 2888.

(3) Schleyer, P.v.R.; Sax, A. F.; Kalcher, J.; Janoschek, R. *Angew. Chem., Int. Ed. Engl.* **1987**, *26*, 364.

(4) Schoeller, W. W.; Dabisch, T.; Busch, T. *Inorg. Chem.* **1987**, *26*, 4383.

(5) Nagase, S.; Kudo, T. *J. Chem. Soc., Chem. Commun.* **1988**, *54*.

(6) Kudo, T.; Nagase, S. *J. Phys. Chem.* **1992**, *96*, 9189.

(7) Dabisch, T.; Schoeller, W. W. *J. Chem. Soc., Chem. Commun.* **1986**, 896.

(8) Kitchen, D. B.; Jackson, J. E.; Allen, L. C. *J. Am. Chem. Soc.* **1990**, *112*, 3408.

(9) Collins, S.; Dutler, R.; Rauk, A. *J. Am. Chem. Soc.* **1988**, *109*, 2564.

(10) See, for example: (a) Nagase, S.; Kudo, T. *Organometallics* **1987**, *6*, 2456. (b) Schleyer, P.v.R.; Janoschek, R. *Angew. Chem., Int. Ed. Engl.* **1987**, *26*, 1267. (c) Sax, A. F.; Kalcher, J. *J. Comput. Chem.* **1989**, *10*, 309. (d) Nagase, S.; Nakano, M. *Angew. Chem., Int. Ed. Engl.* **1988**, *27*, 1081. (e) Nagase, S.; Nakano, M. *J. Chem. Soc., Chem. Commun.* **1988**, 1077.

(11) Jones, R.; Williams, D. J.; Kabe, Y.; Masamune, S. *Angew. Chem., Int. Ed. Engl.* **1986**, *25*, 173.

effects of replacing the bridgehead hydrogens in Si<sub>4</sub>H<sub>6</sub> with methyl and *tert*-butyl groups is examined in this study. (Note that *tert*-butyl groups are present at the bridgehead positions in the experimentally observed derivative.<sup>11</sup>) Furthermore, this work examines the relative energy and isomerization barrier of the bond-stretch isomers of the parent compound using a systematically chosen suite of basis sets and theoretical methods.

### Theoretical Methods

The geometries and energies of the bond-stretch isomers and connecting transition states of tetrasilabicyclo[1.1.0]butane and its 1,3-dimethyl and 1,3-di-*tert*-butyl derivatives were calculated at the generalized valence bond<sup>12</sup> (GVB) level of theory using the 3-21G\* basis set<sup>13,14</sup> (denoted as GVB/3-21G\*). The bonding ( $\sigma$ ) and antibonding ( $\sigma^*$ ) orbitals of the Si–Si bridge bond comprised the single GVB pair.<sup>15</sup> The geometry of each molecule was fully optimized within the confines of the molecular point group symmetry. All stationary points were then verified as local minima or transition states by diagonalizing the matrices of energy second derivatives; i.e., the hessian matrices. The intrinsic reaction coordinate (IRC)<sup>16</sup> connecting each transition state structure to the bond-stretch minima was traced using the Gonzales–Schlegel second-order method.<sup>17</sup> Relative energies were refined via single-point energy calculations with the more flexible 6-31G(d)<sup>14,18a</sup> basis set, using GVB, second-order configuration interaction (SO-CI),<sup>19</sup> and Møller–Plesset second-order perturbation theory (MP2).<sup>20</sup>

The relative energies of the stationary points of the parent molecule Si<sub>4</sub>H<sub>6</sub> were further characterized via single-point energy calculations using a variety of basis sets (6-31G(d,p),<sup>14,18a,c</sup> 6-311G(d,p),<sup>14,18b,c</sup> 6-311++G(d,p),<sup>14,18b-d</sup> 6-311++G-(2df,2pd),<sup>14,18b-d</sup> 6-311G(2d,2p),<sup>14,18b-d</sup> and 6-311G(2df,2pd)<sup>14,18b-d</sup>) and theoretical methods, including GVB, coupled-cluster singles and doubles with an approximate triples correction (CCSD-(T)<sup>21</sup>), MP2, and second-order perturbation corrections from a complete active space wave function (CASPT2).<sup>22</sup>

(12) (a) Goddard, W. A., III; Dunning, T. H.; Hunt, W. J.; Hay, P. J. *Acc. Chem. Res.* **1973**, *6*, 368. (b) Bobrowicz, F. W.; Goddard, W. A., III. *Modern Theoretical Chemistry*; Schaefer, H. F., III, Ed.; Plenum Press: New York, 1977; Vol 3.

(13) (a) Binkley, J. S.; Pople, J. A.; Hehre, W. J. *J. Am. Chem. Soc.* **1980**, *102*, 939. (b) Gordon, M. S.; Binkley, J. S.; Pople, J. A.; Pietro, W. J.; Hehre, W. J. *J. Am. Chem. Soc.* **1982**, *104*, 2797.

(14) Gordon, M. S. *Chem. Phys. Lett.* **1980**, *76*, 163.

(15) This wave function is also known as a two-configuration self-consistent field (TCSCF) or a two-electron, two-orbital multiconfigurational SCF ([2e,2o] MCSCF) wave function.

(16) (a) Ishida, K.; Morokuma, K.; Komornicki, A. *J. Chem. Phys.* **1977**, *66*, 2153. (b) Muller, K. *Angew. Chem., Int. Ed. Engl.* **1980**, *19*, 1. (c) Schmidt, M. W.; Gordon, M. S.; Dupuis, M. *J. Am. Chem. Soc.* **1985**, *107*, 2585. (d) Garrett, B. C.; Redmon, M. J.; Steckler, R.; Truhlar, D. G.; Baldrige, K. K.; Bartol, D.; Schmidt, M. W.; Gordon, M. S. *J. Phys. Chem.* **1988**, *92*, 1476. (e) Baldrige, K. K.; Gordon, M. S.; Steckler, R.; Truhlar, D. G. *J. Phys. Chem.* **1989**, *93*, 5107.

(17) (a) Gonzales, C.; Schlegel, H. B. *J. Phys. Chem.* **1990**, *94*, 5523. (b) Gonzales, C.; Schlegel, H. B. *J. Chem. Phys.* **1991**, *95*, 5853.

(18) (a) Ditchfield, R.; Hehre, W. J.; Pople, J. A. *J. Chem. Phys.* **1971**, *54*, 724. Hehre, W. J.; Ditchfield, R.; Pople, J. A. *J. Chem. Phys.* **1972**, *56*, 2257. (b) Krishnan, R.; Binkley, J. S.; Seeger, R.; Pople, J. A. *J. Chem. Phys.* **1980**, *72*, 650. McLean, A. D.; Chandler, G. S. *J. Chem. Phys.* **1980**, *72*, 5639. (c) Hariharan, P. C.; Pople, J. A. *Theoret. Chim. Acta* **1972**, *28*, 213. Fracl, M. M.; Pietro, W. J.; Hehre, W. J.; Binkley, J. S.; Gordon, M. S.; DeFrees, D. J.; Pople, J. A. *J. Chem. Phys.* **1982**, *77*, 3654. (d) Frisch, M. J.; Pople, J. A.; Binkley, J. S. *J. Chem. Phys.* **1984**, *80*, 3265.

(19) The SOCI wave function consists of all configurations arising from single and double electronic excitations from the one-pair GVB wave function.

(20) (a) Møller, C.; Plesset, M. S. *Phys. Rev.* **1934**, *46*, 618. (b) Bartlett, R. J. *Annu. Rev. Phys. Chem.* **1981**, *32*, 359. (c) Pople, J. A.; Binkley, J. S.; Seeger, R. *Int. J. Quantum Chem.* **1976**, *S10*, 1.

(21) (a) Ragavachari, K.; Trucks, G. W.; Head-Gordon, M.; Pople, J. A. *Chem. Phys. Lett.* **1989**, *157*, 479. (b) Bartlett, R. J.; Watts, J. D.; Kucharski, A.; Noga, J. *Chem. Phys. Lett.* **1990**, *165*, 513; **1990**, *167*, 609.

All GVB and SOCI calculations were performed using the *ab initio* electronic structure program GAMESS.<sup>23</sup> The MP2 and CCSD(T) calculations were done using GAUSSIAN92,<sup>24</sup> and the CASPT2 calculations were performed using the MOLCAS-2<sup>25</sup> program.

### Results and Discussion

For ease of discussion, the short bond isomer, the long bond isomer, and the connecting transition-state structure of the parent compound, Si<sub>4</sub>H<sub>6</sub>, will be referred to as [1<sub>SB</sub>], [1<sub>LB</sub>], and [1<sub>TS-A</sub>], respectively. An additional transition-state structure, which connects the bond-stretch isomers but also effects ring inversion, is similar to one found for the 1,3-disilabicyclo[1.1.0]butane (Si<sub>2</sub>C<sub>2</sub>H<sub>6</sub>) analog<sup>2</sup> and is denoted as [1<sub>TS-B</sub>]. Likewise, the corresponding structures of the 1,3-dimethyl (1,3-di-*tert*-butyl) derivative will be denoted as [2<sub>SB</sub>], [2<sub>LB</sub>], [2<sub>TS-A</sub>], and [2<sub>TS-B</sub>] ([3<sub>SB</sub>], [3<sub>LB</sub>], [3<sub>TS-A</sub>], and [3<sub>TS-B</sub>]), respectively.

**A. Geometries.** The salient geometrical parameters of the GVB/3-21G\* optimized structures of [1], [2], and [3] are summarized in Table 1.<sup>26</sup> The main structural features which differentiate the bond-stretch stationary points are the Si–Si bridge bond length, the X–Si–Si angle (X = H, CH<sub>3</sub>, or ((CH<sub>3</sub>)<sub>3</sub>C), and the dihedral angle defined by the four silicon atoms ( $R_{13}$ ,  $\alpha_{513}$ , and  $\omega$  in Table 1, respectively.)

As can be seen in Table 1, the geometry of the silicon atom framework of the short bond isomers is nearly independent of the bridgehead substituents. Specifically,  $R_{13}$  is approximately 2.38 Å, the peripheral Si–Si bond length  $R_{12}$  is about 2.30 Å,  $\alpha_{513}$  is in the range 146–150°, and  $\omega$  is in the range 118–120° for all three short bond structures. Although  $R_{12}$  is consistently between 2.33 and 2.34 Å in the long bond minima, there is somewhat more variation in the other long bond geometrical parameters; i.e.,  $2.9 \text{ \AA} < R_{13} < 3.1 \text{ \AA}$ ,  $90^\circ < \alpha_{513} < 118^\circ$ , and  $139^\circ < \omega < 150^\circ$ . Therefore, the geometries of the long bond isomers are more sensitive to the bridgehead groups than are the short bond structures.

GVB/3-21G\* Si<sub>4</sub>H<sub>6</sub> transition-state structures [1<sub>TS-A</sub>] and [1<sub>TS-B</sub>] and the imaginary mode displacement vectors (shown leading to the long bond isomer) are depicted in Figure 1. The corresponding GVB/3-

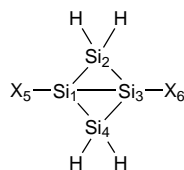
(22) (a) Andersson, K.; Malmqvist, P.-A.; Roos, B. O.; Sadlej, A. J.; Wolinski, K. *J. Phys. Chem.* **1990**, *94*, 5483. (b) Andersson, K.; Malmqvist, P.-A.; Roos, B. O. *J. Chem. Phys.* **1992**, *96*, 1218. (c) Andersson, K.; Roos, B. O. *Int. Quantum Chem.* **1993**, *45*, 591.

(23) (a) Dupuis, M.; Spangler, D.; Wendoloski, J. J. *NRCC Software Catalog* **1980**, *1*, Program QG01. (b) Schmidt, M. W.; Boatz, J. A.; Baldrige, K. K.; Koseki, S.; Gordon, M. S.; Elbert, S. T.; Lam, B. *QCPE* **1987**, *7*, 115. (c) Schmidt, M. W.; Baldrige, K. K.; Boatz, J. A.; Jensen, J. H.; Koseki, S.; Gordon, M. S.; Nguyen, K. A.; Windus, T. L.; Elbert, S. T. *QCPE* **1990**, *10*, 52. (d) Schmidt, M. W.; Baldrige, K. K.; Boatz, J. A.; Elbert, S. T.; Gordon, M. S.; Jensen, J. H.; Koseki, S.; Matsunaga, N.; Nguyen, K. A.; Su, S.; Windus, T. L. *J. Comput. Chem.* **1993**, *14*, 1347.

(24) Frisch, M. J.; Trucks, G. W.; Head-Gordon, M.; Gill, P. M. W.; Wong, M. W.; Foresman, J. B.; Johnson, B. G.; Schegel, H. B.; Robb, M. A.; Replogle, E. S.; Gomperts, R.; Andres, J. L.; Ragavachari, K.; Binkley, J. S.; Gonzales, C.; Martin, R. L.; Fox, D. J.; Defrees, D. J.; Baker, J.; Stewart, J. J. P.; Pople, J. A. Gaussian 92, Gaussian, Inc., Pittsburgh, PA, 1992.

(25) Andersson, K.; Fulscher, M. P.; Lindh, R.; Malmqvist, P.-A.; Olsen, J.; Roos, B. O.; Sadlej, A. J.; Widmark, P.-O. *MOLCAS Version 2, User's Guide*; University of Lund: Lund, Sweden, 1991.

(26) Complete GVB/3-21G\* geometries for [1<sub>SB</sub>], [1<sub>TS-A</sub>], and [1<sub>LB</sub>] are presented in ref 2. Complete geometries, harmonic vibrational frequencies, and IR intensities for all structures are available upon request.

**Table 1.** GVB/3-21G\* Structures

structures <sup>a</sup> for X = H (point group)				
param	[1 <sub>SB</sub> ] <sup>b</sup> (C <sub>2v</sub> )	[1 <sub>TS-A</sub> ] <sup>b</sup> (C <sub>2v</sub> )	[1 <sub>TS-B</sub> ] <sup>b</sup> (C <sub>2v</sub> )	[1 <sub>LB</sub> ] <sup>b,c</sup> (C <sub>2v</sub> )
R <sub>13</sub>	2.380	2.512	2.932	2.912 (2.840)
R <sub>12</sub>	2.302	2.288	2.325	2.331 (2.327)
R <sub>15</sub>	1.478	1.476	1.483	1.490 (1.492)
α <sub>513</sub>	146.1	128.7	-174.5 <sup>f</sup>	90.3 (90.3)
ω	120.0	133.7	147.9	139.0 (140.0)

structures <sup>a</sup> for X = CH <sub>3</sub> (point group)				
param	[2 <sub>SB</sub> ] <sup>b</sup> (C <sub>2v</sub> )	[2 <sub>TS-A</sub> ] <sup>b</sup> (C <sub>2v</sub> )	[2 <sub>TS-B</sub> ] <sup>b</sup> (C <sub>2v</sub> )	[2 <sub>LB</sub> ] <sup>d</sup> (C <sub>s</sub> )
R <sub>13</sub>	2.383	2.600	2.993	2.989
R <sub>12</sub>	2.304	2.288	2.330	2.335
R <sub>23</sub>				2.338
R <sub>15</sub>	1.894	1.904	1.901	1.920
R <sub>36</sub>				1.917
α <sub>513</sub>	148.6	125.9	-167.7 <sup>f</sup>	99.3
α <sub>631</sub>				101.0
ω	118.0	137.5	150.0	141.0

structures <sup>a</sup> for X = C(CH <sub>3</sub> ) <sub>3</sub> (point group)				
param	[3 <sub>SB</sub> ] <sup>b,g</sup> (C <sub>2v</sub> )	[3 <sub>TS-A</sub> ] <sup>e</sup> (C <sub>2</sub> )	[3 <sub>TS-B</sub> ] <sup>b</sup> (C <sub>2v</sub> )	[3 <sub>LB</sub> ] <sup>e</sup> (C <sub>2</sub> )
R <sub>13</sub>	2.383 (2.373)	2.651	2.954	3.061
R <sub>12</sub>	2.305 (2.335)	2.292	2.327	2.338
R <sub>23</sub>	(2.310)	2.291		2.341
R <sub>15</sub>	1.907	1.924	1.912	1.934
α <sub>513</sub>	149.9	125.9	-168.3 <sup>f</sup>	117.7
ω	117.7 (121)	139.0	146.7	149.8

<sup>a</sup> Bond lengths in angstroms, angles in degrees.  $R_{ab}$ ,  $\alpha_{abc}$ , and  $\omega$  denote the distance between atoms a and b, the angle defined by atoms a, b, and c, and the dihedral angle defined by the four silicon atoms, respectively. <sup>b</sup> Since these structures have C<sub>2v</sub> symmetry,  $R_{12} = R_{14} = R_{23} = R_{34}$ ,  $R_{15} = R_{36}$ , and  $\alpha_{513} = \alpha_{631}$ . <sup>c</sup> MP2/6-31G(d,p) optimized values given in parentheses. <sup>d</sup> Since this structure has C<sub>s</sub> symmetry,  $R_{12} = R_{14}$  and  $R_{23} = R_{34}$ . <sup>e</sup> Since these structures have C<sub>2</sub> symmetry,  $R_{12} = R_{34}$ ,  $R_{23} = R_{14}$ , and  $\alpha_{513} = \alpha_{631}$ . <sup>f</sup> See text. <sup>g</sup> Experimental structure<sup>11</sup> given in parentheses. The  $R_{12}$  ( $R_{23}$ ) value in parentheses is the average of the experimental  $R_{12}$  and  $R_{34}$  ( $R_{14}$  and  $R_{23}$ ) bond lengths from ref 11.

21G\* transition-state structures for the dimethyl [2] and di-*tert*-butyl [3] derivatives are shown in Figures 2 and 3, respectively. The isomerization transition states [1<sub>TS-A</sub>], [2<sub>TS-A</sub>], and [3<sub>TS-A</sub>] are all qualitatively similar in that their geometries are approximately midway between their corresponding bond stretch minima (see Table 1). Relative to the long bond isomers, there is somewhat less variation in the structures of the isomerization transition states (1<sub>TS-A</sub>), [2<sub>TS-A</sub>], and [3<sub>TS-A</sub>].  $R_{12}$  is consistently about 2.29 Å, and  $2.5 < R_{13} < 2.7$  Å,  $126^\circ < \alpha_{513} < 129^\circ$ , and  $134^\circ < \omega < 139^\circ$ . IRC calculations, which trace the minimum energy path from a transition state to reactants and products, have been performed to verify that each of the "isomerization-only" TS-A transition states connect the corresponding bond stretch minima.<sup>27</sup>

(27) Since [2<sub>LB</sub>] has C<sub>s</sub> symmetry, the IRC starting from [2<sub>TS-A</sub>] (which has C<sub>2v</sub> symmetry) does not directly lead to the long bond minimum. Rather, the IRC trace leads to a C<sub>2v</sub> stationary point which is virtually identical in structure to [2<sub>LB</sub>] but with the methyl hydrogens in an eclipsed conformation. This conformation has one imaginary vibrational frequency corresponding to internal rotation of a methyl group and lies only 0.2 kcal/mol above [2<sub>LB</sub>]. Similar comments apply to the IRC trace connecting [3<sub>TS-B</sub>] and [3<sub>LB</sub>].

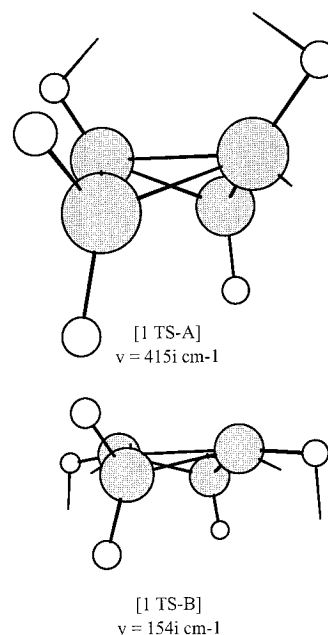


**Figure 1.** GVB/3-21G\* transition-state structures connecting the bond-stretch isomers of [1]. Silicon and hydrogen atoms are denoted as shaded and open circles, respectively. The normal mode displacement vector corresponding to the imaginary frequency (given below each structure) is shown in the direction leading to the long bond isomer.

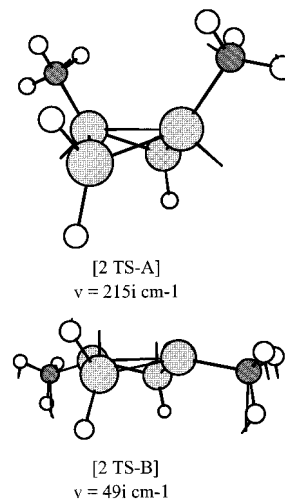


**Figure 2.** GVB/3-21G\* transition-state structures connecting the bond-stretch isomers of [2]. Silicon, carbon and hydrogen atoms are denoted as lightly shaded, darkly shaded, and open circles, respectively. The normal mode displacement vector corresponding to the imaginary frequency (given below each structure) is shown in the direction leading to the long bond isomer.

The combination isomerization/ring-inversion transition-state structures [1<sub>TS-B</sub>], [2<sub>TS-B</sub>], and [3<sub>TS-B</sub>] are markedly different from the "isomerization-only" TS-A saddle points. The most striking feature is the folding of the bridgehead substituent underneath the silicon atom framework (see Figures 1–3). This is denoted in Table 1 by negative values of  $\alpha_{513}$ . For [1<sub>TS-B</sub>] and [2<sub>TS-B</sub>],  $R_{13}$  is actually slightly longer than in the corresponding long bond isomer while for [3<sub>TS-B</sub>]  $R_{13}$  is about 0.1 Å shorter than in [3<sub>LB</sub>]. The three TS-B structures are qualitatively similar, with  $R_{12}$  approximately equal to 2.33 Å,  $2.93 < R_{13} < 2.99$  Å,  $-175^\circ <$

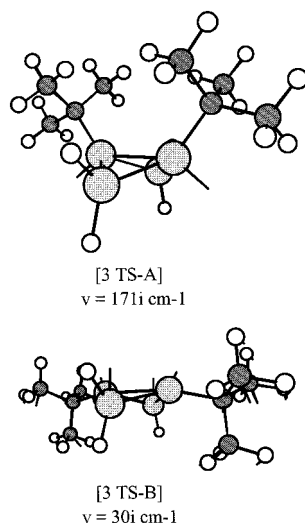


**Figure 3.** GVB/3-21G\* transition-state structures connecting the bond-stretch isomers of [3]. Silicon, carbon, and hydrogen atoms are denoted as lightly shaded, darkly shaded, and open circles, respectively. The normal mode displacement vector corresponding to the imaginary frequency (given below each structure) is shown in the direction leading to the long bond isomer.

**Table 2.** Natural Orbital Occupation Numbers<sup>a</sup>

	SB	TS-A	TS-B	LB
		[1]		
$\sigma$	1.951	1.940	1.633	1.827
$\sigma^*$	0.033	0.040	0.360	0.163
		[2]		
$\sigma$	1.952	1.931	1.664	1.827
$\sigma^*$	0.031	0.049	0.328	0.163
		[3]		
$\sigma$	1.952	1.921	1.645	1.794
$\sigma^*$	0.031	0.059	0.348	0.195

<sup>a</sup> SOCI/6-31G(d)//GVB/3-21G\* level.

$\alpha_{513} < -167^\circ$ , and  $139^\circ < \omega < 150^\circ$ . IRC traces of the minimum energy path were used to verify that each of the "TS-B" saddle points not only connect the bond stretch minima but also lead to inversion of the silicon ring system.<sup>27</sup>

Included in Table 1 is the experimental X-ray structure of the silicon framework of the 1,3-di-*tert*-butyl-2,2,4,4-tetrakis(2,6-diethylphenyl) derivative,<sup>11</sup> which has approximate  $C_2$  symmetry and for which only the short bond structure is observed. Since this derivative is chemically most closely related to [3], the experimental structure is compared to the predicted geometry of [3<sub>SB</sub>]. The calculated bridge bond length  $R_{13}$  in [3<sub>SB</sub>] is 0.01 Å longer than that in the diethylphenyl derivative. The difference between the computed and observed Si-Si peripheral bond lengths  $R_{12}$  and  $R_{23}$  is somewhat greater, with the calculated values being 0.01–0.03 Å shorter than in the observed structure.

**B. Electronic Structure.** Table 2 summarizes the SOCI/6-31G(d) natural orbital occupation numbers of the bridgehead Si-Si bonding ( $\sigma$ ) and antibonding ( $\sigma^*$ ) pair orbitals in the GVB wave function for each local minimum and saddle point. For [1<sub>SB</sub>], the  $\sigma$  and  $\sigma^*$  occupation numbers (1.95 and 0.03, respectively) show a slightly larger occupation of the antibonding orbital compared to a typical Si-Si single bond. For example, in disilane at the same level of theory, the Si-Si  $\sigma$  and  $\sigma^*$  occupation numbers are 1.97 and 0.01, respectively.

**Table 3.** Relative Energies of R<sub>2</sub>Si<sub>4</sub>H<sub>4</sub> Bond-Stretch Isomers<sup>a</sup>

level	SB	TS-A	TS-B	LB
		[1]		
GVB/3-21G*	0.0 (0.0)	2.1 (2.0)	9.5 (9.1)	-9.6 (-9.7)
GVB/6-31G(d)	0.0 (0.0)	1.1 (1.0)	6.4 (6.0)	-12.4 (-12.5)
SOCI/6-31G(d)	0.0 (0.0)	1.3 (1.2)	10.2 (9.8)	-10.1 (-10.1)
MP2/6-31G(d)	0.0 (0.0)	-1.8 (-1.9)	17.5 (17.1)	-9.8 (-9.9)
		[2]		
GVB/3-21G*	0.0 (0.0)	6.3 (6.3)	11.0 (10.7)	-1.9 (-2.0)
GVB/6-31G(d)	0.0 (0.0)	4.5 (4.5)	7.5 (7.2)	-4.5 (-4.6)
SOCI/6-31G(d)	0.0 (0.0)	5.1 (5.1)	15.0 (14.7)	-1.8 (-1.9)
MP2/6-31G(d)	0.0 (0.0)	0.8 (0.8)	18.0 (17.7)	-3.2 (-3.3)
		[3]		
GVB/3-21G*	0.0 (0.0)	7.2 (6.9)	10.4 (9.7)	4.9 (4.6)
GVB/6-31G(d)	0.0 (0.0)	6.0 (5.7)	7.9 (7.2)	2.5 (2.2)
SOCI/6-31G(d)	0.0 (0.0)	6.8 (6.5)	11.7 (11.0)	5.1 (4.8)
MP2/6-31G(d)	0.0 (0.0)	0.6 (0.3)	17.5 (16.8)	2.4 (1.7)

<sup>a</sup> Energies in kcal/mol, ZPE-corrected energies in parentheses. All energies are computed using the GVB/3-21G\* geometries.

The  $\sigma^*$  orbital in [1<sub>LB</sub>], with an occupation number of nearly 0.2, is more heavily populated than in [1<sub>SB</sub>]. The simple isomerization saddle point [1<sub>TS-A</sub>] has an intermediate  $\sigma^*$  occupation of 0.04. However, the combination isomerization/inversion structure [1<sub>TS-B</sub>] has the largest degree of diradical character, with a  $\sigma^*$  occupation of 0.36 electron. Although the  $\sigma$  orbital has the dominant population in all four structures, there is clearly a significant level of diradical character present in these systems. However, none are dominantly diradical in nature, which would be manifested by nearly equal  $\sigma$  and  $\sigma^*$  occupations. The same conclusions can be drawn for the dimethyl and di-*tert*-butyl derivatives, which show similar patterns in their  $\sigma$  and  $\sigma^*$  occupation numbers.

**C. Energies.** Table 3 shows the relative energies of the bond-stretch isomers and their connecting transition states as a function of bridgehead substituent. (A negative relative energy means that the long bond structure is the more thermodynamically stable isomer.) For the parent compound [1], the long bond isomer is lower in energy than the short bond structure by about 10 kcal/mol, at the GVB/3-21G\* level of theory. The energetic preference for [1<sub>LB</sub>] remains at 10 kcal/mol at the SOCI/6-31G(d) and MP2/6-31G(d) levels and actually increases slightly to 12 kcal/mol at the GVB/6-31G(d) level.

The isomerization barrier to formation of [1<sub>LB</sub>] via the simple isomerization saddle point [1<sub>TS-A</sub>] is only 2 kcal/mol at the GVB/3-21G\* level and decreases to only 1 kcal/mol at the GVB/6-31G(d) and SOCI/6-31G(d) levels. However, the barrier vanishes at the MP2/6-31G(d) level, which suggests the possibility that the short bond isomer of [1] is not a local minimum at the MP2 level (*vide infra*). This suggests that the parent compound [1] does not exhibit bond-stretch isomerism but rather exists as a single structure with an elongated Si-Si bridge bond. The predicted barrier to formation of [1<sub>LB</sub>] by way of the combination isomerization/ring inversion saddle point [1<sub>TS-B</sub>] is substantially higher than via [1<sub>TS-A</sub>], ranging from approximately 6 kcal/mol (GVB/6-31G(d)) to over 17 kcal/mol (MP2/6-31G(d)).

Replacement of the bridgehead hydrogens with methyl groups decreases the energetic preference of the long bond isomer to approximately 2–5 kcal/mol (see Table 3). This is consistent with the results of Nagase and Kakano<sup>10c</sup> but in contrast to two other earlier theoretical

**Table 4. Total and Relative Energies of Si<sub>4</sub>H<sub>6</sub> Bond-Stretch Isomers and Transition-State "A"<sup>a,b</sup>**

level of theory	SB	TS-A	LB
GVB/3-21G*	-1153.333 05 (0.0)	-1153.329 66 (2.1)	-1153.348 36 (-9.6)
GVB/6-31G(d)	-1159.090 53 (0.0)	-1159.088 76 (1.1)	-1159.110 35 (-12.4)
GVB/6-31G(d,p)	-1159.098 99 (0.0)	-1159.097 20 (1.1)	-1159.118 44 (-12.2)
GVB/6-311G(d,p)	-1159.178 79 (0.0)	-1159.176 46 (1.5)	-1159.196 97 (-11.4)
GVB/6-311++G(d,p)	-1159.179 62 (0.0)	-1159.177 25 (1.5)	-1159.197 79 (-11.4)
GVB/6-311++G(2df,2pd)	-1159.200 53 (0.0)	-1159.197 46 (1.9)	-1159.215 13 (-9.2)
MP2/6-31G(d)	-1159.413 19 (0.0)	-1159.416 04 (-1.8)	-1159.428 84 (-9.8)
MP2/6-31G(d,p)	-1159.460 28 (0.0)	-1159.463 01 (-1.7)	-1159.475 90 (-9.8)
MP2/6-311G(d,p)	-1159.562 07 (0.0)	-1159.564 20 (-1.3)	-1159.577 36 (-9.6)
MP2/6-311G(2d,2p)	-1159.604 24 (0.0)	-1159.604 83 (-0.4)	-1159.617 72 (-8.5)
MP2/6-311G(2df,2pd)	-1159.669 47 (0.0)	-1159.670 43 (-0.6)	-1159.680 13 (-6.7)
CCSD(T)/6-31G(d)	-1159.488 33 (0.0)	-1159.491 05 (-1.7)	-1159.504 67 (-10.3)
CCSD(T)/6-31G(d,p)	-1159.536 77 (0.0)	-1159.539 35 (-1.6)	-1159.553 01 (-10.2)
CCSD(T)/6-311G(d,p)	-1159.642 85 (0.0)	-1159.644 86 (-1.3)	-1159.658 71 (-10.0)
CCSD(T)/6-311G(2d,2p)	-1159.689 24 (0.0)	-1159.689 68 (-0.3)	-1159.702 87 (-8.6)
CCSD(T)/6-311G(2df,2pd)	-1159.757 56 (0.0)	-1159.758 26 (-0.4)	-1159.768 09 (-6.6)
CASPT2/6-31G(d) <sup>c</sup>	-1159.450 69 (0.0)	-1159.456 52 (-3.7)	-1159.472 33 (-13.6)
CASPT2/6-31G(d) <sup>d</sup>	-1159.453 97 (0.0)	-1159.456 67 (-1.7)	-1159.472 22 (-11.5)

<sup>a</sup> Optimized GVB/3-21G\* geometries. <sup>b</sup> Total energies in hartrees, relative energies (in parentheses) in kcal/mol. <sup>c</sup> Energy obtained using diagonal one-particle operator.<sup>22</sup> <sup>d</sup> Energy obtained using nondiagonal one-particle operator.<sup>22</sup>

studies<sup>3,4</sup> which predict [**2**<sub>LB</sub>] to be less stable than [**2**<sub>SB</sub>]. The barrier to formation of [**2**<sub>LB</sub>] via the simple isomerization saddle point [**2**<sub>TS-A</sub>] is higher than for the unsubstituted compound and does not vanish at the MP2/6-31G(d) level, although the predicted MP2 barrier is less than 1 kcal/mol. As in the case of [**1**], the barrier to formation of the long bond isomer via the combination isomerization/ring inversion saddle point is higher than via the simple isomerization transition state, ranging from 7.5 kcal/mol at the GVB/6-31G(d) level to 18 kcal/mol at the MP2/6-31G(d) level.

*tert*-Butyl groups at the bridgehead positions actually reverse the order of relative stability, leading to a 2–5 kcal/mol energy preference for the short bond isomer. Note that although the bridgehead *tert*-butyl groups raise the energy of the long bond isomer above the short bond minimum, the long bond isomer remains a local minimum on the potential energy surface, at the GVB/3-21G\* level. However, MP2/6-31G(d) predicts the simple isomerization transition state [**3**<sub>TS-A</sub>] to lie about 2 kcal/mol *below* the long bond isomer; i.e., isomerization to the short bond isomer via [**3**<sub>TS-A</sub>] occurs without a barrier and so the long bond isomer presumably is not a local minimum. As in the case of the parent system [**1**], this result suggests that [**3**] does not exhibit bond stretch isomerism. Unlike [**1**], however, the single local minimum of [**3**] is the one with a "normal" Si–Si bridge bond length. This is consistent with the experimental X-ray crystal structure<sup>11</sup> of a diethylphenyl derivative of [**3**], where only the short bond isomer is observed. The barrier to formation of the short bond isomer via [**3**<sub>TS-B</sub>] is again higher than via the simple isomerization saddle point [**3**<sub>TS-A</sub>], ranging from 5 kcal/mol at the GVB and SOCI levels to 15 kcal/mol at the MP2 level.

Solely on the basis of steric interactions between the bridgehead groups, one might expect the relative stability of the long bond isomer to increase as the bulkiness of the bridgehead substituents increases. Since the distance between the bridgehead silicon atoms in the long bond isomer is greater than in the short bond counterpart, it seems reasonable that there should be less steric crowding at the bridgehead positions in the long bond structure. However, the data in Table 3 show just the opposite trend in relative stability. This seemingly counterintuitive effect can be understood by examining in more detail the bond-stretch geometries

of the parent compound, which are summarized in Table 1. While the bridgehead Si–Si internuclear distance is indeed larger in [**1**<sub>LB</sub>] than in [**1**<sub>SB</sub>] (2.91 Å vs 2.38 Å), the bridgehead hydrogen atoms in [**1**<sub>LB</sub>] are nearly 2 Å closer together than they are in [**1**<sub>SB</sub>]. The reason for this is the markedly smaller bridgehead H–Si–Si angle in [**1**<sub>LB</sub>] relative to that in [**1**<sub>SB</sub>]. Therefore, the preference for a small bridgehead angle in the long bond isomer suggests that its relative stability will decrease as the size of the bridgehead groups increases. This is consistent with the data in Table 3.

Further evidence for increased steric crowding in the long bond isomers is found by examining the point group symmetries of the bond stretch stationary points, which are found in Table 1. For the parent compound, all four stationary points have *C*<sub>2v</sub> symmetry. In the dimethyl derivative, the short bond isomer as well as both saddle point structures also have *C*<sub>2v</sub> symmetry, with the methyl groups in an eclipsed conformation. However, in the long bond structure [**2**<sub>LB</sub>], the *C*<sub>2v</sub> conformation is no longer a local minimum but rather has one imaginary vibrational frequency, whose associated normal mode describes internal rotations of the methyl groups about the Si–C bonds. This is a result of the more severe steric crowding in the long bond isomer, which precludes an eclipsed conformation of the methyl groups. Consequently, [**2**<sub>LB</sub>] has reduced symmetry (*C*<sub>s</sub>) in which the methyl groups are in a staggered arrangement. In the di-*tert*-butyl derivative, the bridgehead substituents are sufficiently bulky that only the short bond minimum and the combination isomerization/ring inversion transition state retain *C*<sub>2v</sub> symmetry. The steric repulsion between the *tert*-butyl groups in the simple isomerization saddle point and the long bond isomer is sufficient to distort the molecular symmetry to *C*<sub>2</sub>.

A more thorough examination of the relative energies of the Si<sub>4</sub>H<sub>6</sub> bond stretch minima and the connecting saddle point [**1**<sub>TS-A</sub>] as a function of basis set and theoretical method is summarized in Table 4. Single-pair GVB single point calculations using the 6-31G(d), 6-31G(d,p), 6-311G(d,p), 6-311++G(d,p), and 6-311++G(2df,2pd) basis sets consistently predict the long bond isomer [**1**<sub>LB</sub>] to be 9–12 kcal/mol more stable than the short bond structure. Likewise, the GVB energies

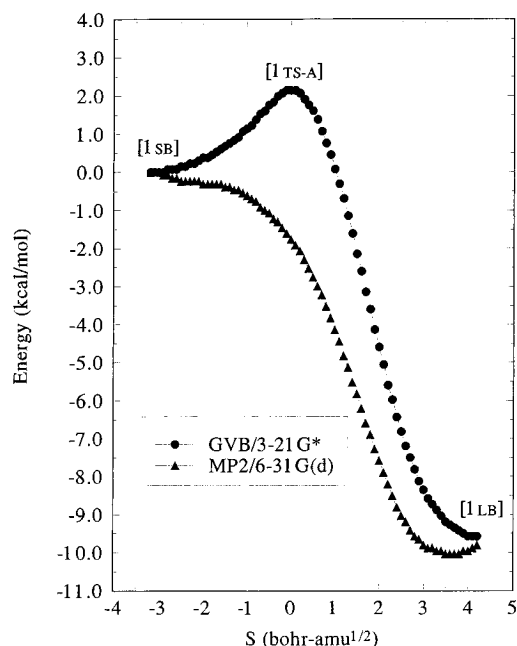


**Figure 4.** GVB/3-21G\* (circles) and MP2/6-31G(d) (triangles) relative energies along the GVB/3-21G\* IRC connecting  $[1_{SB}]$  and  $[1_{LB}]$  via  $[1_{TS-A}]$ . The  $[1_{SB}]$ ,  $[1_{TS-A}]$ , and  $[1_{LB}]$  stationary points are located at  $S = -3.2$ ,  $0.0$ , and  $4.2$  bohr  $\text{amu}^{1/2}$ , respectively.

consistently predict the transition state  $[1_{TS-A}]$  to lie approximately 1–2 kcal/mol above  $[1_{SB}]$ .

However, a different picture emerges at the MP2 and CCSD(T) levels. Although  $[1_{LB}]$  is again consistently predicted to be more stable than  $[1_{SB}]$ , the predicted energetic preference for  $[1_{LB}]$  is slightly less (7–10 kcal/mol) than in the GVB calculations. Even more importantly, at the MP2 and CCSD(T) levels the transition state  $[1_{TS-A}]$  lies *below* the short bond isomer by 0.5–2 kcal/mol. This suggests the possibility that there exists only a single local minimum (namely, the long bond structure) at the MP2 and CCSD(T) levels of theory. To further investigate this possibility, MP2/6-31G(d) single-point energies were computed at several points on the GVB/3-21G\* IRC connecting the bond-stretch isomers  $[1_{SB}]$  and  $[1_{LB}]$  via  $[1_{TS-A}]$ . Figure 4 shows the GVB/3-21G\* and MP2/6-31G\*(d) energies as a function of the mass-weighted distance  $S$  along the IRC,<sup>16</sup> where it is clearly seen that at the MP2/6-31G(d) level there is no barrier separating the bond-stretch isomers. Additionally, an MP2/6-31G(d,p) geometry optimization of the short bond isomer, starting at the GVB/3-21G\* geometry, was performed. The MP2 optimization led to the long bond structure, which a subsequent MP2 hessian calculation predicted to be a local minimum. Thus, at both the MP2/6-31G(d) and MP2/6-31G(d,p) levels, it appears that only the long bond structure is a local minimum. The MP2/6-31G(d,p) optimized structure of  $[1_{LB}]$  is summarized in Table 1. Although the MP2 Si–Si bridge bond length (2.840 Å) is substantially shorter than the GVB/3-21G\* value (2.912 Å), the remaining geometric parameters are in excellent agreement.

In light of the nontrivial degree of diradical character present in  $[1]$  (*vide supra*), CASPT2 single point energies (using the GVB pair orbitals as the active space) were computed as a check of the reliability of the single-configuration-based MP2 and CCSD(T) results, with the results summarized in Table 4. The CASPT2 relative

energies are nearly identical to the MP2 and CCSD(T) results, thus confirming the notion that the short bond isomer is not a local minimum. (This is consistent with the study by Busch et al.,<sup>28</sup> who were unable to locate the  $\text{Si}_4\text{H}_6$  short bond isomer at the MCSCF/DZP level.) Therefore, it appears that  $[1_{LB}]$  is the only minimum and  $[1_{TS-B}]$  is actually a simple ring inversion saddle point.

## Conclusions

This theoretical study has examined the effects of methyl and *tert*-butyl bridgehead substitution on the relative energies of the bond-stretch isomers and their connecting transition states of  $\text{Si}_4\text{H}_6$ . The long bond isomers are more sensitive to steric crowding at the bridgehead positions. Methyl substitution at both bridgehead positions lowers the energetic preference for the long bond isomer from about 10 kcal/mol in the parent compound to less than 5 kcal/mol. The order of relative stability is reversed in the di-*tert*-butyl derivative, with the short bond isomer more stable by 2–5 kcal/mol.

At the GVB/3-21G\* level, two transition states connecting the bond-stretch isomers are found for each tetrasilabicyclobutane derivative. One of these saddle points (TS-A) follows a straightforward isomerization pathway, while the other (TS-B) leads to inversion of the silicon ring system in addition to bond-stretch isomerism. The barrier to isomerization via TS-A is smaller than via TS-B for all three compounds.

For the parent compound  $[1]$ , MP2, CCSD(T), and CASPT2 single-point energy calculations predict the long bond isomer to be the only local minimum. The good agreement among these three methods for  $\text{Si}_4\text{H}_6$  suggests MP2 is quite reliable for the methyl- and *tert*-butyl-substituted compounds as well. For the dimethyl derivative  $[2]$ , MP2/6-31G(d) single-point calculations predict the existence of both bond-stretch isomers, with the long bond structure more stable by 3 kcal/mol, but separated by a barrier of less than 1 kcal/mol. Therefore, it is possible that a more refined level of theory would predict the existence of only the long bond isomer, as in the case of  $[1]$ . Replacement of the bridgehead hydrogens with *tert*-butyl groups reverses the order of stability of the bond stretch isomers, with the short bond isomer lower in energy by 2–5 kcal/mol. MP2/6-31G(d) single-point energy calculations predict no barrier to formation of the short bond isomer  $[3_{SB}]$ , and thus the long bond isomer  $[3_{LB}]$  apparently is not a local minimum at this level. This is consistent with the experimental structure of the diethylphenyl derivative of  $[3]$ , where only the short bond isomer is observed.

Prior to the present study, the existence of bond-stretch isomerism in silicon analogs of bicyclobutanes has been largely unresolved. In this paper, high-quality calculations are used to illustrate unequivocally that bond-stretch isomerism does not exist for the simplest parent species or for a substituted compound similar to the only tetrasilabicyclo compounds that has been synthesized to date. The structure for the substituted and unsubstituted species are expected to be rather different (short bond as observed experimentally and

(28) Busch, T.; Esposti, A. D.; Werner, H.-J. *J. Chem. Phys.* **1991**, *94*, 6708.

long bond, respectively). Although bond-stretch isomers may very well not exist for any of the compounds considered here, a bridgehead substituent of intermediate size (e.g., methyl) is the most likely candidate for the observation of bond-stretch isomerism.

**Acknowledgment.** The research was supported in part by a grant of high-performance computing time from the Department of Defense on the IBM SP2 located at the Maui High Performance Computing Center. This study was also performed in part using the Intel Touchstone Delta System (operated by Caltech on behalf

of the Concurrent Supercomputing Consortium). Access to the Touchstone Delta System was provided by the Advanced Research Projects Agency (ARPA). Some of the calculations were carried out on IBM RS6000 workstations generously provided by Iowa State University and on a Cray Y-MP at the San Diego Supercomputer Center. This work was supported in part by a grant from the Air Force Office of Scientific Research (F49620-95-1-0077). The authors thank Ms. Galina Chaban for computational assistance.

OM9508501